Finite Element Modeling and Simulation of Substation Porcelain Insulator Posts Subjected to Earthquake Loading

M.A. Moustafa, K.M. Mosalam
*University of California, Berkeley*

15 WCEE
LISBOA 2012

SUMMARY

The study presented in this paper focused on developing accurate computational finite element (FE) model and conducting numerical simulations of a single disconnect switch porcelain insulator post. Developed FE model was calibrated using experiments that were previously conducted by the authors. The simulations included linear and nonlinear static and dynamic analyses. First, eigenvalue analysis was performed to evaluate the vibration properties. Next, static linear and nonlinear pushover analyses were performed. Several material characterization test results were utilized to calibrate the nonlinear material model. The model parameters were varied to conduct a sensitivity study that focused on ranking sources of uncertainties in insulator modelling using a "Tornado diagram" representation. Finally, dynamic analyses were carried out using a simulated earthquake signal. The magnitude of the applied signal was increased until dynamic failure occurred, and the dynamic failure load was compared to the corresponding static value.

Keywords: Earthquake loading, electric equipment, finite element analysis, porcelain insulator.

1. INTRODUCTION

Insulator posts are key components of electrical disconnect switches and main parts of many electrical equipment used in power transmission and distribution systems. A focused research effort to study the seismic behavior of electrical switches is needed because of the severe damage that the electrical switches in general, and insulator posts in particular, have experienced over the past years during many earthquakes inside and outside the United States. The damage during an earthquake can be either limited to the brittle porcelain insulator components, or it can be extended to the whole switch (Fujisaki, 2009). Examples of porcelain insulator failures and consequent failures of switches are shown in Fig. 1.1.
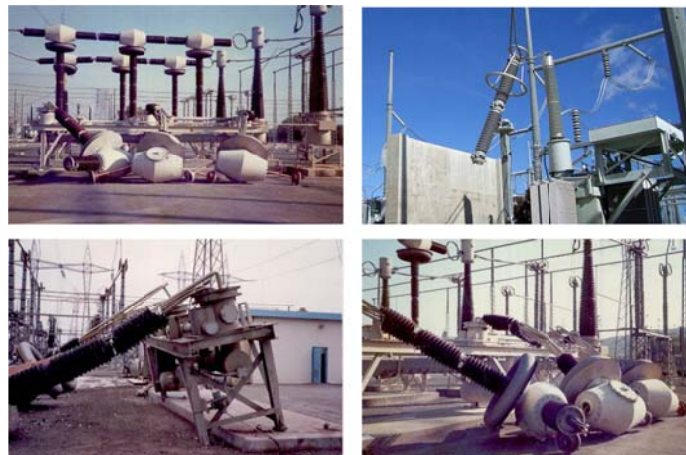
Figure 1.1 Failure examples of porcelain insulators after earthquakes (Fujisaki, 2009).

Since only few studies considered seismic behavior of the insulators posts of disconnect switches (Gilani et al., 2000 and Takhirov et al., 2004), the study presented herein focused only on a single 230-kV insulator post. That was to develop a better understanding of the insulators seismic behavior through finite element (FE) modeling and simulations. The first main objective was to conduct a sensitivity study to rank the different sources of uncertainties in insulator FE modeling and how the insulator behavior at failure is affected by the modeling parameters and assumptions. The dynamic failure of the insulator post was not possible to achieve experimentally (Mosalam et al., 2012). Thus, nonlinear dynamic analysis was sought to determine global insulator failure behavior under earthquake loading as a second objective.

Several computational models were developed and calibrated using relevant experimental and material tests. However, only the most accurate FE model is presented herein. The conducted FE analyses included eigenvalue modal analysis, linear and nonlinear static and dynamic analyses. The nonlinear static (pushover) analysis focused on ranking the sources of uncertainties in insulator modeling through an extensive parametric study. Different model parameters were varied based on previously conducted material tests and the failure load and displacement were determined for each case. A "tornado diagram" was used to rank the sources uncertainties in model parameters.

The most accurate nonlinear FE model calibrated from static analysis was used to conduct dynamic analysis using a base excitation similar to a signal applied to 230-kV sub-structured tests in a study conducted by the authors (Mosalam et al., 2012). The base excitation was applied at different scales to capture when the insulator failed under dynamic loading. Thus, it was possible to obtain the corresponding dynamic nonlinear force-displacement relationship for a single porcelain insulator post that is used in 230-kV electrical disconnect switches.

2. EXPERIMENTAL RESULTS

Several experiments were conducted by the authors (Mosalam et al., 2012) on single 230-kV porcelain insulator post. The experimental results were utilized in developing and calibrating the FE computational models. A brief discussion of the relevant tests used in this paper is presented in this section. First, several impact hammer tests were conducted on the insulator post in both of the static and dynamic test configurations for natural frequency determination. In the static test configuration, the insulator was connected to the reaction frame through a rigid base plate, and the mean value of frequency was found to be 19.25 Hz. On the other hand, the insulator had a frequency of 12.77 Hz when it was connected to the shaking table through a relatively flexible base plate in the dynamic test configuration. The difference in frequency is attributed to the flexibility difference at the insulator base in each test setup.

Several ramp cyclic-loading tests were conducted in the static configuration to obtain the force-displacement relationship and to estimate the insulator lateral stiffness. From the different runs, an average stiffness of 1.61 kips/in. was determined for the single insulator post. Subsequently, the insulator top was pulled to failure (fragility test) directly after the last applied load cycle to determine the mode of failure and the values of force and displacement at failure. The insulator had a very brittle mode of failure at 2.23 kips and corresponding displacement 1.60 inch. However, since the fragility was conducted right after several cyclic tests without letting the force to drop to zero after the cyclic tests, it was desired to shift the fragility curve to a zero starting point to facilitate FE model calibration and comparisons. This led to a corresponding failure load of 2.6 kips.

The broken insulator parts were used to prepare six cylindrical specimens, Fig. 2.1, for porcelain characterization. The material tests aimed at determining the porcelain density, Young's modulus, Poisson's ratio, compressive strength, and tensile strength. These material properties were used to accurately calibrate the porcelain material model in the FE model. Several specimens were used such that the variation in the determined properties was utilized to vary the porcelain nonlinear material model parameters in the sought sensitivity analysis and parametric study.

Another test used in the FE model calibration was the shaking table test of the 230-kV insulator post. The considered dynamic test was one of many tests conducted to demonstrate the concept of sub-structuring in vertical-break disconnect switches (Mosalam et al., 2012). The 230-kV insulator dynamic tests were conducted on a unidirectional shaking table at the structures laboratory of UC-Berkeley. Since the studied insulator is typically a part of the disconnect switch mounted on top of a support structure, the use of ground motion was not suitable for dynamic testing. Instead, a signal was generated from the accelerations measured on top of the switch support structure from a previous full switch seismic qualification test (Mosalam et al., 2012). The measured accelerations on the unidirectional shaking table were used for base excitation in the dynamic FE analyses, and responses were compared for FE model calibration.
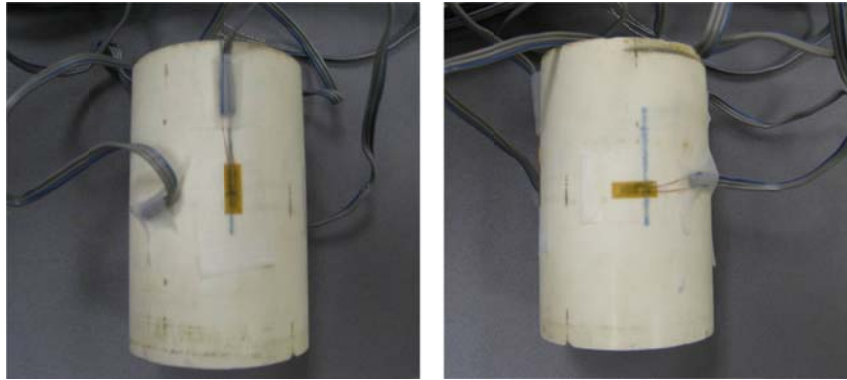

Figure 2.1 Sample of porcelain cylinders used in material tests and instrumented to determine Young's modulus (left) and Poisson's ratio (right).

3. FE MODEL DESCRIPTION AND CALIBRATION

In order to achieve an accurate FE model for the 230-kV porcelain insulator post, several computational models were developed using both SAP2000 (2009) and DIANA (2008) FE Analysis (FEA) packages. Only the most accurate DIANA model, designated as M7, is used in this paper and the reader is referred to (Mosalam et al. 2012) for full discussion of all FE models and simulations.

3.1. Model Description

The DIANA M7 model was the most accurate FE model. It accounted for the exact geometry of the tested porcelain insulator post. In addition, this model accurately presented the metallic caps and their connections to the porcelain core through cementitious grout layers. The accurate modeling of such connection is motivated by the fact that most of previously tested insulators fractured and failed near the porcelain-metal interface (Takhirov et al., 2009). The model geometry and FE mesh, shown in Fig. 3.1, were generated using FX+; a pre- and post-processor of DIANA. The model used 4-node tetrahedron solid elements.
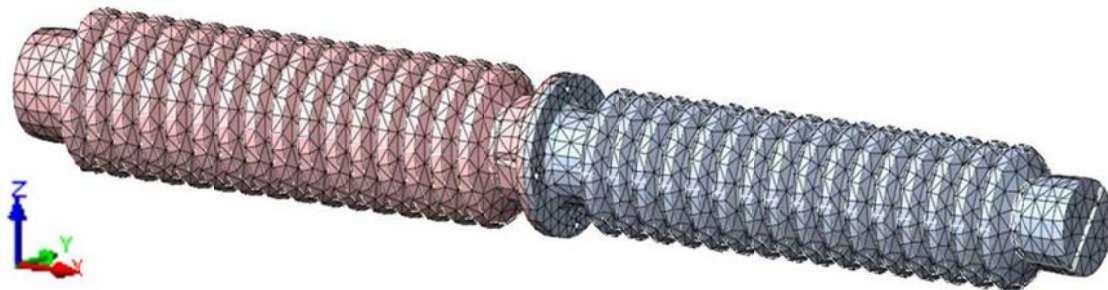
Figure 3.1 DIANA M7 finite element model and mesh for the 230-kV porcelain insulator post.

Three different materials were needed in the FE model to define the mechanical properties, namely cementitious grout, porcelain, and cast iron. Linear elastic material models were defined for the cementitious grout and cast iron using typical properties available from literature. However, due to the porcelain rupture and brittle failure, a nonlinear material model was used for the porcelain. The "Total Strain Rotating Crack" nonlinear material model available in DIANA was adopted. The porcelain model parameters were determined from the previously mentioned material characterization tests. The variation in the properties resulting from several porcelain specimens was very useful in varying the model parameters in the conducted sensitivity study.

3.2. Model Calibration

In order to calibrate the FE model, eigenvalue, linear static and linear dynamic analyses were conducted and results were compared against the experimental results.

3.2.1. Eigenvalue Analysis
The natural frequency computed from DIANA eigenvalue analysis was compared to the experimental value determined from the impact hammer tests. The computational fundamental frequency of 20.40 Hz reasonably agreed with the 19.25 Hz experimental value (error = 6%). Fig. 3.2 shows the first mode shape obtained from DIANA M7 model eigenvalue analysis.
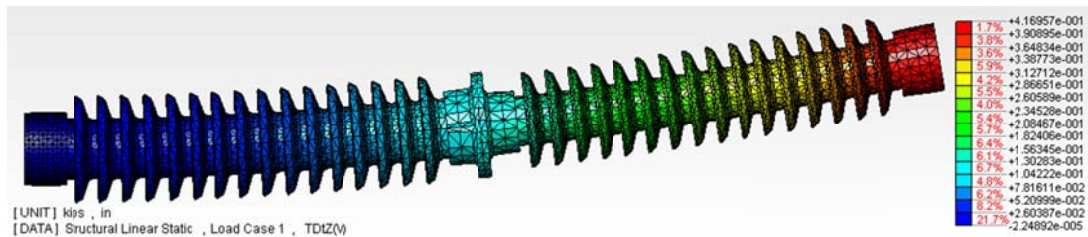
Figure 3.2 First mode shape for DIANA model M7 (frequency = 20.4 Hz).

3.2.2. Linear Static Analysis
Linear static analysis using the insulator computational model was conducted to estimate the lateral stiffness to compare it to the experimentally estimated stiffness. An equivalent unit surface load was applied at the cantilever tip, and the corresponding nodal displacements were determined, Fig. 3.3.
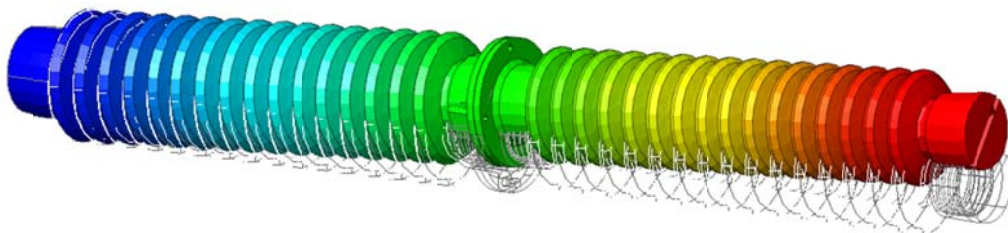
Figure 3.3 Typical deformed shape of FE model due to static analysis using unit tip force.

The FE model adopted a full fixation at all the nodes at the base to represent the very stiff base plate connection used in the static tests of the 230-kV insulator. The stiffness value from the FE model was determined as 1.98 kips/in., which is higher than the experimental value of 1.61 kips/in. This variation is expected because of the full base fixation introduced in the FEA, in addition to the variability in the material properties.

3.2.3. Linear Dynamic Analysis
The FE model used in the eigenvalue and static analyses was modified using tension-only springs at the insulator base for more accurate modeling of the base flexibility. The dynamic test configuration used a much flexible connection at the insulator base than the static configuration. The springs used a

bilinear behavior with infinite stiffness in compression and calibrated value in tension. The infinite compression stiffness was meant to reflect the fact that the metallic cap at insulator base cannot penetrate through the base plate. However, the bolts can stretch when tensioned which in turn introduce rotations at the insulator base.

The flexible boundaries reduced the model stiffness, and hence reduced the fundamental frequency. A second eigenvalue analysis was conducted and the fundamental frequency from the modified FE model was determined. The new computational frequency was 12.84 Hz versus 12.77 Hz determined from the impact hammer tests when the insulator was mounted on the shaking table in the dynamic test setup. Achieving a comparable computational frequency value was necessary to proceed with the dynamic analysis.

As mentioned previously at the end of Section 2, the accelerations measured at the insulator base on the shaking table during the 100%-scale test were employed as the excitation for the linear FEA. The FE dynamic analysis results were very comparable to the experimental results. That good match gave confidence about using the FE model in nonlinear dynamic analyses. Complete discussion of the dynamic analysis results and comparisons can be found in (Mosalam et al., 2012).

4. RANKING UNCERTAINTIES IN PORCELAIN INSULATOR MODELING

After calibrating the computational model, displacement-controlled nonlinear static analyses (0.05 in. increments applied at the insulator tip until failure) were performed. Subsequently, a sensitivity study was conducted to study how the force (cantilever load) and displacement at failure are affected by changing one of the FE model parameters, e.g. the porcelain tensile strength. In other words, since each model parameter reflects a source of uncertainty (or a random variable), it was intended to rank these sources of uncertainties to determine which parameter affects the modeled insulator response more. A "tornado analysis", similar to that in (Lee and Mosalam, 2005), was used in this study.

Several features of the DIANA M7 model influenced the nonlinear analysis and parametric study. Full capability of nonlinear material model was utilized for porcelain, i.e. not only the Young's modulus definition as was the case in linear analyses and model calibration. Reduction in the grout Young's modulus value was considered to account for any grout separation and/or degradation due to micro-cracking that might develop at failure. The boundary condition at the base defined by bilinear springs contributed to the nonlinear behavior of the model.

4.1. Sources of Uncertainties

The FE model was used to investigate the sensitivity of the response of the insulator computational model to different input parameters that reflect sources of uncertainties in modeling. Each source of uncertainty (random variable) does not have a deterministic value, but have a range of possible values.

Five sources of uncertainties (parameters) were considered in conducting the incremental nonlinear static (pushover) analysis. One input parameter was varied at a time while the remaining four parameters were held constant at their mean values. The first three parameters were related to the nonlinear porcelain material model and include: Young's Modulus (E_p), tensile strength (f_t) and fracture energy density (g_f). The conducted material tests showed large variability in these properties and governed the varied material model parameters. The fourth source of uncertainty was the value used to calibrate the stiffness of the bilinear base springs in tension. The four springs represented the bolts used to attach the insulator base to the support structure. The corresponding variation can be a result of using different bolt lengths or different bolt alloy. Three different bolt lengths, 0.5, 1.0, and 1.5 in. were used for the spring stiffness in tension calibration. The last parameter considered was the possible degradation and/or separation in the grout layer at the contact surface between the porcelain core and the metallic flange (cap). In order to avoid a computationally expensive FE model, a linear elastic material model was used for the grout layer. However, different levels of grout micro-cracking were considered by using Young's modulus values ranging from 100% to 10% of the initial value.

To study the sensitivity of the modeled insulator post to each of the above mentioned parameters independently, five groups of models were used. In each group, only one parameter was varied and the remaining four parameters were held constant at their mean values. Fourteen combinations, and in turn 14 models, forming the 5 groups A to E were sought to conduct the parametric (sensitivity) study.

4.2. Parametric Study Results

The nonlinear static analysis involved applying a total tip displacement of 2.5 inch in 50 steps (0.05 inch increments). The corresponding force at the base was determined to obtain the force-displacement relationship. The analysis was repeated for all 14 models, and the obtained force-displacement relationships were compared to the fragility pull test results. Five families of force-displacement relationships were obtained corresponding to the considered 5 groups. Only the one obtained by varying the porcelain Young's modulus (E_p) is presented here in Fig. 4.1 as a sample of the results. However, a summary of failure loads and corresponding displacements obtained for each of the 14 different models is shown in Table 4.1. These values were used to evaluate the range of change in response corresponding to each of the studied sources of uncertainties for the sake of the tornado diagram analysis as discussed next.
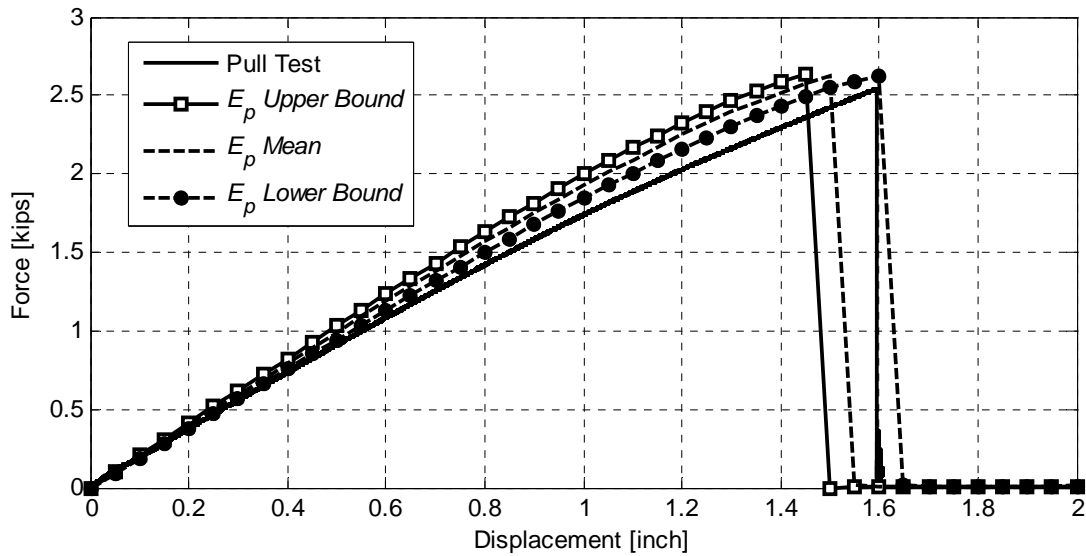

**Figure 4.1** Force-displacement relationships when varying Ep only (Group D).

Table 4.1 Parametric study results.

| Group	Variable Parameter	Model	Failure Load [kips]	Disp. at Failure Load [inch]
A	g_f	M7- B1	2.813	1.60
		M7- B2	2.072	1.05
		M7- B3	1.720	0.85
		M7- B4	1.041	0.50
B	E_g	M7- B5	2.648	1.45
		M7- B6	2.651	1.50
		M7- B7	2.621	1.50
		M7- B8	2.605	1.60
C	k_s	M7- B9	2.628	1.60
		M7- B10	2.611	1.40
D	E_p	M7- B11	2.633	1.45
		M7- B12	2.621	1.60
E	f_t	M7- B13	3.082	1.70
		M7- B14	2.218	1.35

4.3. Tornado Diagram Analysis

The tornado diagram, commonly used in decision analysis, is an effective way to represent the effect of sources of uncertainties. It has been recently used in sensitivity analysis in earthquake engineering and probabilistic seismic evaluation of structural components and systems (Lee and Mosalam, 2005). The tornado diagram consists of a set of horizontal bars, referred to as swings, one for each source of uncertainty (random variable). The length of each swing represents the variation in the output due to the variation in the respective parameter. Thus, a variable with larger effect on the output has larger swing than those with lesser effect. In a tornado diagram, swings are displayed in the descending order of the swing size from the top to the bottom. This wide-to-narrow arrangement of swings eventually resembles the shape of a tornado.

In this study, the output of each tornado diagram is one of the porcelain insulator response quantities. These are the failure load and corresponding displacement. Typically in a tornado diagram analysis, the deterministic function is evaluated twice, using the two extreme values of the selected input random variable, while the other input random variables are set to their best estimates such as the medians. The conducted nonlinear FE analysis of the single porcelain insulator post is considered to be the deterministic function evaluation in this study. In addition, each of the 5 groups of parameters that ranged between upper and lower bounds represented the input to the FE analysis. When one of the input parameters (variables) was set to a lower or upper bound, the rest of parameters (variables) were set to the mean values as previously mentioned. In this case, the two bounding values of the output can be obtained directly for each of the 5 groups from Table 4.1 that summarizes the failure load and displacement (output) values for each run (variable input). The absolute difference of these two values is the swing of the output corresponding to the selected input random variable. The tornado is then built by arranging the obtained swings in a descending order as mentioned above, and the sources of uncertainties are ranked accordingly according to its influence. The tornado diagram for the first output which was the failure load is shown in Fig. 4.2, while that for the displacement at failure is shown in Fig. 4.3. The tornado diagrams in these figures present a clear picture of the effecting parameter identification, where the Young's modulus (E_p) and tensile strength (f_t) are observed to have significant effect on the response compared to the others
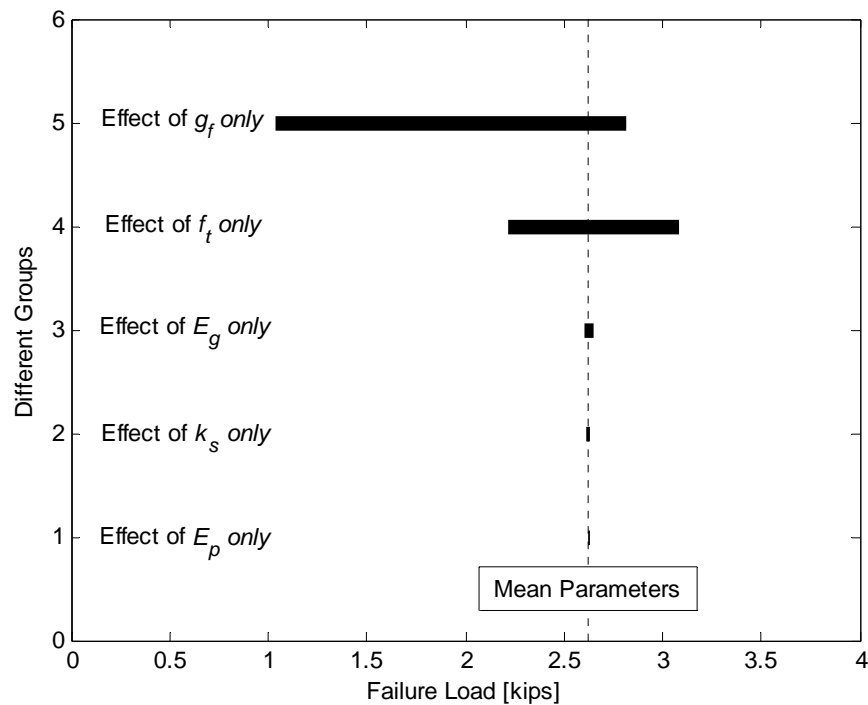
Figure 4.2 Tornado diagram for the effect of different sources of uncertainties on the failure load.
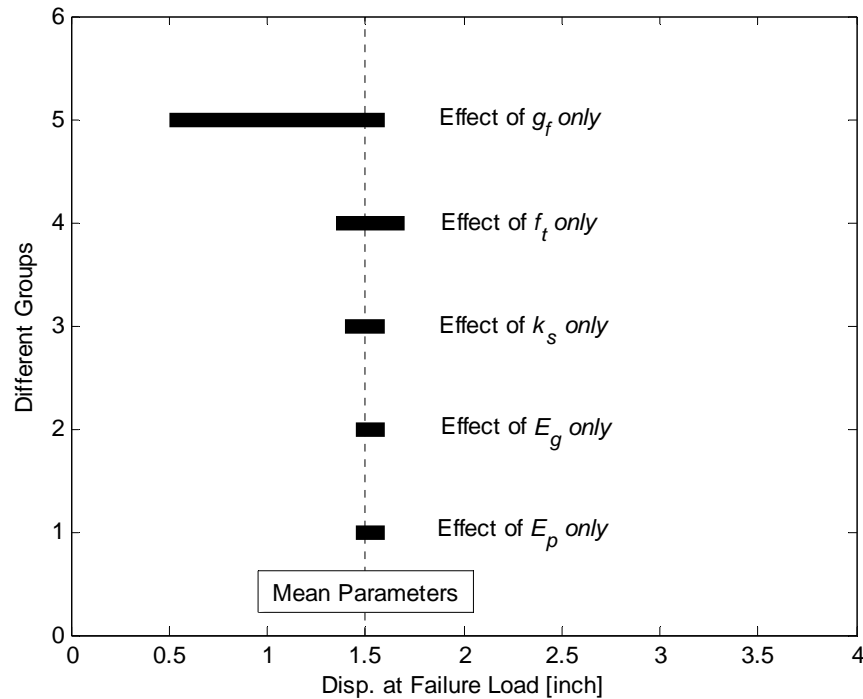
Figure 4.3 Tornado diagram for the effect of different sources of uncertainties on failure displacement.

## 5. NONLINEAR DYNAMIC ANALYSIS

The nonlinear dynamic analysis used one of the DIANA M7 models of the previous parametric study, namely M7-BM12 in Table 4.1. This model considered the lower bound for the porcelain Young's modulus and the mean values for the rest of the model parameters and showed the best match with experimental force-displacement relationship. For computational efficiency, the nonlinear analysis considered only the strong motion part of the signal. A 5-second signal comprising the peak acceleration was used. The main objective of the nonlinear dynamic analysis was to understand the nature of the insulator failure under dynamic loading, which was not possible to determine experimentally due to the shaking table limitations.

It should be noted that the accelerations measured on the unidirectional shaking table was used only in linear dynamic analysis for model calibration purposes using the test results. However, for all the nonlinear dynamic analyses, the input signal generated directly from support structure response, as mentioned in Section 2, was used since it represents a more realistic loading in terms of the nonlinear response evaluation of the insulator. This is because the input signal does not contain the possible noise and amplification introduced by the dynamic characteristics of the unidirectional shaking table.

The strong motion part of the signal was applied with increasing scale until failure was captured. The first global failure and instability was observed when the signal was 10 times amplified. As shown in Fig. 5.1, the relative displacement at insulator top increased significantly. The peak value for the relative displacement at this scale was unrealistically large indicating a global failure. Therefore, scale 9 signal was considered as the maximum intensity level that the insulator can withstand before global failure. The peak values of several response parameters, namely top acceleration, displacement (total and relative), base force and number of cracks opened during the analysis, were determined (Mosalam et al., 2012). A summary of these peak values at the end of each analysis run is presented in Table 5.1. The peak input acceleration is also presented in Table 5.1.

To determine the failure load from the obtained results, the peak force–peak displacement relationship, Fig. 5.2, was developed. The relationship is almost linear until failure, which agrees with the brittle

behavior expected from the porcelain insulator. The failure load is suggested to be the last point on the linear portion of the relationship before extremely large displacements were observed, i.e. a failure load of 5.76 kips. The determined dynamic failure load of 5.76 kips was 2.2 times the load capacity determined from nonlinear static analysis of the same M7-BM12 model (failed at 2.62 kips from Table 4.1, which was very close to the actual value obtained from fragility test). The reason why the force capacity determined from dynamic loading is almost double the value from the static loading is attributed to the distributed mass, and in turn distributed force, along the insulator height. In a static configuration, the load is applied at the insulator top leading to a large moment arm that is equal to the entire insulator height. However, in a dynamic test, the base moment is equal to the integral of the product of the distributed mass, acceleration and varying moment arm, which in turn results in a reduced moment arm for the resultant force and this explains the reduced base moment values and obtained higher load capacity.
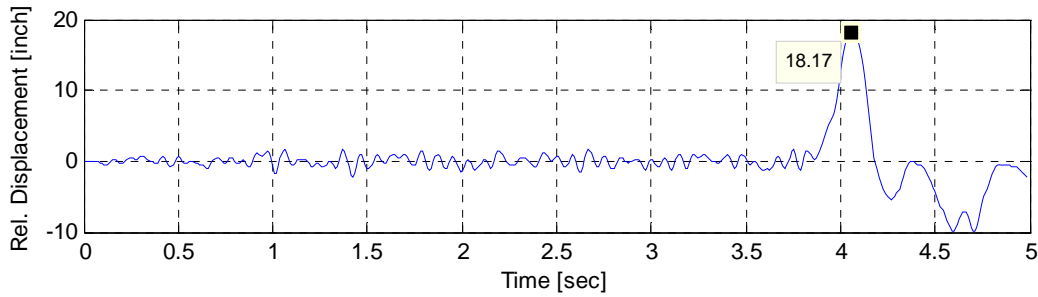
Figure 5.1 The relative displacement time history at insulator top for scale 10 signal.

Table 5.1 Peak values of response quantities at different input signal levels from the dynamic analyses.

Input Signal		Peak Force [kips]	Peak Top Acceleration [g] (ratio with peak input acceleration)	Peak Total Disp. [in.]	Peak Relative Disp. [in.]	Number of opened cracks
Scale	Peak Acc. [g]					
1	1.65	0.64	3.86 (2.34)	3.43	0.27	0
2	3.30	1.43	7.73 (2.34)	6.86	0.55	0
3	4.95	2.15	15.02 (3.03)	10.15	0.73	87
4	6.60	2.90	20.95 (3.17)	13.38	1.01	932
5	8.25	3.64	28.49 (3.45)	16.62	1.29	2859
7	11.55	4.78	33.17 (2.87)	23.14	1.60	8878
9	14.85	5.76	37.67 (2.54)	29.75	2.00	22958
10	16.50	6.29	40.96 (2.48)	33.52	18.17	45671
11	18.15	7.60	56.77 (3.13)	53.02	76.76	70782

6. CONCLUDING REMARKS

The following conclusions can be inferred from the presented FE computational investigation of porcelain post insulators of the 230-kV substation vertical disconnect switches:

1) The close agreement between the FE analyses results and the experimental values provided confidence of the validity and accuracy of the adopted detailed DIANA finite element model.

2) In the conducted sensitivity analysis to rank the sources of uncertainties in the porcelain insulator computational modeling, two model parameters were found to be significantly affecting the failure load and the corresponding displacement values. These parameters are the porcelain fracture energy density and tensile strength. Therefore, a reliable FE computational model should account for these uncertainties in the porcelain material properties, in cases where it is not possible to eliminate them physically.

3) Only the porcelain fracture energy density (g_f), as a source of uncertainty, was found to affect the values of the insulator failure load and displacements together without affecting the model initial stiffness. On the other hand, all other sources of uncertainty affected either the failure load or displacement independently, which indicates a change in the model initial stiffness.

4) The failure load and mode of failure of the porcelain insulator under earthquake loading was determined using nonlinear dynamic FEA, since it was not possible to fail the insulator in dynamic testing. The determined dynamic failure load was 2.2 times the load capacity determined from static fragility tests and calibrated nonlinear static analysis because of the distributed mass of the insulator that leads to distributed forces along insulator height.

5) A proper amplification factor has to be utilized if the dynamic failure load is to be estimated from a cantilever static test. A suggested amplification factor of 2 is recommended for the case of the 230-kV porcelain insulator posts based on the ratio determined from the calibrated static and dynamic FE simulations in this study.
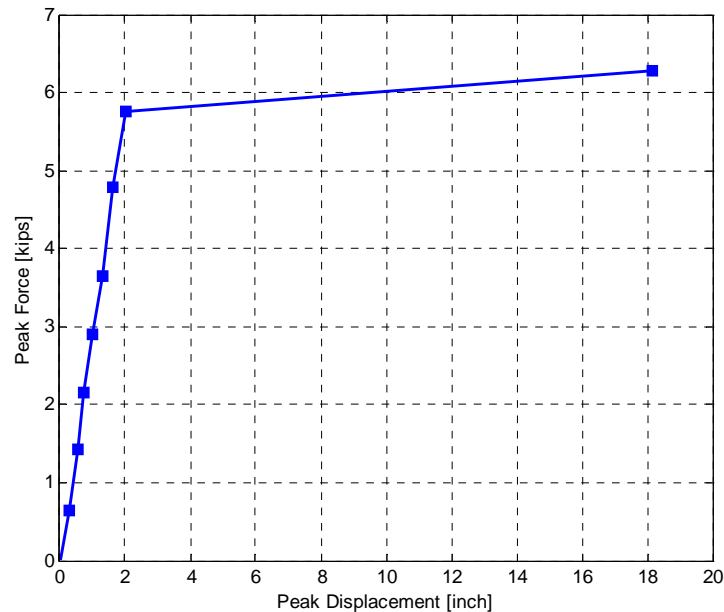
Figure 5.2 Peak force versus peak displacement relationship from nonlinear dynamic analyses

REFERENCES

DIANA, 2008. Finite Element Analysis User's Manual 9.3, TNO DIANA BV, The Netherlands.
Fujisaki, E. 2009. Seismic Performance of Electric Transmission Systems, Conference Presentation, *PEER Annual Meeting, San Francisco, California*.
Gilani, A.S.J., Whittaker, A.S., Fenves, G.L., Chen, C.-H., Ho, H. and Fujisaki, E. 2000. Seismic Evaluation and Analysis of 230-kV Disconnect Switches. Pacific Earthquake Engineering Research Center, Report 2000/06. PEER, University of California, Berkeley.
Lee T.-H. and Mosalam K.M., 2005. Seismic Demand Sensitivity of Reinforced Concrete Shear-Wall Building Using FOSM Method. *Earthquake Engineering and Structural Dynamics*, Vol. 34, No. 14, 1719-1736.
Mosalam, K.M., Moustafa, M.A., Günay, M.S., Triki, I. and Takhirov, S. 2012. Seismic Performance of Substation Insulator Posts for Vertical-Break Disconnect Switches. California Energy Commission Publication Number: CEC-500-2012.
SAP2000. 2009. Version 14, Analysis Reference Manual, Computer and Structures, Inc., Berkeley, CA.
Takhirov, S., Fenves, G. and Fujisaki, E. 2004. Seismic Qualification and Fragility Testing of Line Break 550-kV Disconnect Switches. Pacific Earthquake Engineering Research Center, Report 2004/08. PEER, University of California, Berkeley.
Takhirov, S., Schiff, A., Kempner, L. and Fujisaki, E. 2009. Breaking Strength of Porcelain Insulator Sections Subjected to Cyclic Loading. *TCLEE-2009 Proceedings, Oakland, California*.